New backstepping controllers with enhanced stability for neutral point clamped converters interfacing photovoltaics and AC microgrids

J. Dionísio Barros[a,*], dbarros@uma.pt, J. Fernando A. Silva[b], Luis Rocha[c]

[a]University of Madeira, INESC-ID, Campus Universitário da Penteada, 9020-105 Funchal, Portugal

[b]Instituto Superior Técnico, University of Lisbon, INESC-ID, Av. Rovisco Pais, 1049-001 Lisboa, Portugal

[c]Instituto Superior de Engenharia de Lisboa, Polytechnic Institute of Lisbon, INESC-ID, Rua Conselheiro Emídio Navarro, 1959-007 Lisboa, Portugal

*Corresponding author.

Abstract

This work presents a new approach to obtain pulse width modulation (PWM) backstepping controllers with enhanced stability for neutral point clamped (NPC) multilevel converters to deliver energy from photovoltaic (PV) panels into AC microgrids. Stability enhanced backstepping non-linear controllers are obtained from the equations of the *dq* frame converter model to regulate the PV voltage to track the power point, and to balance the capacitor voltages through DC biasing of the PWM carriers, using a novel dynamic equation of the capacitors incremental unbalance voltage, while controlling the grid injected AC currents. Besides, the proposed controllers can change the PV panels operating point to curtail inject power for AC voltage / frequency regulation. The NPC converter and AC microgrid are simulated in MATLAB / Simulink and implemented in the laboratory to evaluate the performance of the PV energy conversion using the new stability enhanced backstepping PWM control. Simulation and experimental results show that, regarding predictive controllers, the novel stability enhanced backstepping requires lower microprocessor power than predictive controllers while presenting a similar behavior in PV voltage and power point tracking regulation, or for voltage / frequency regulation of the microgrid. AC injected currents show low levels of total harmonic distortion similar to predictive controllers and can operate at near unity power factor .

Keywords: Energy conversion; PV; Microgrids; Stability enhanced backstepping controller; ~~Multilevel converter~~; NPC; Pulse width modulation

Data availability

No data was used for the research described in the article.

1 Introduction

The penetration of microgrids is growing in the world, due to their ability to include decentralized renewable energy generation and independent (off-line) operation from existing AC grids. Microgrids can incorporate distributed renewable generation sources, such as solar photovoltaic (PV) or wind turbines, together with community energy storage devices (usually battery banks) and therefore can be disconnected from AC distribution grids. Microgrids will be capable of independently solve local power issues, ensuring the quality and reliability of the power supply [1–3].

Globally, electricity consumption continues to grow. It is expected that this growth will continue in coming years, through industrial and human activities, the use of electric cars and the decarbonization of the energy sector. A major

effort is in progress to use distributed energy sources, emphasizing those that are based on renewable energies [4–5].

The main task of switching converters connected to microgrids is to manage the energy flow while ensuring the required electric power quality: on the AC side when delivering AC power, the converter should reduce harmonic distortion on the AC side and maximize the energy transfer efficiency when connected to a load while regulating the DC voltage level on the DC side [6–8].

Considering that AC power networks are now well developed, today the concept of hybrid microgrids (AC / DC) is attracting great interest, due to the presence of DC power sources, photovoltaic panels, fuel cells, electric vehicle (EV) batteries possibility to supply power to the grid (Vehicle to Grid - V2G), and DC loads. Hybrid AC / DC microgrids that have AC / DC loads and sources are considered as the most likely systems for the distribution and electric power transmission [9].

The control of the power / frequency and voltage / frequency of microgrids with distributed inverter-based generators is generally based on the droop control method. This method usually performs well in reactive power regulation but may present some disadvantages in the presence of non-linear loads and may exhibit deviations in frequency regulation. However, hierarchical control, using droop method as primary control, can be applied to AC and DC microgrids to integrating renewable and distributed energy resources and improving the frequency regulation [10–13].

The increasingly use of EVs during the last years indicates that their storage batteries might be employed for the control of power / frequency in microgrids. EVs batteries fitted with bi-directional power converters and controllers can be seen as mobile storage devices able to charge other EVs, with urgent energy needs at high power, or to improve performance of micro-districts [14–15].

The electronic power conversion of microgrids may involve power values in the order of several megawatts at voltages reaching kilovolt levels. Multilevel converters, like NPCs, may be the appropriate solution for kV level microgrids, despite requiring DC capacitor voltage balance. Besides allowing working voltages and power levels suitable for microgrids, multilevel converters allow the improvement of their power quality [16–19].

Feedback controllers, such as Proportional Integral (PI), usually show sensitivity to system parameters and can become unstable with constant power loads [20]. Complex controllers, such as predictive controllers, need much higher speed microprocessors than PIs and fast sampling data devices. In this research work, a new control algorithm is proposed whose stability is not strong dependent on system parameters, while being fast, therefore not requiring high speed microprocessors or fast sampling devices.

The design of controllers for non-linear systems subject to unknown disturbances is the most attractive challenge in the control of microgrids. Non-linear techniques based on the Lyapunov direct method of stability [21] are powerful tools for designing stable and fast controllers for non-linear systems. Needed control quantities and controllers are designed considering slow output DC variables [22–24] and then going to the faster variables up to the control input. As DC voltages have very slow variations while AC currents have fundamental frequencies near 50 Hz, the new stability enhanced backstepping controllers are compared to non-linear controllers obtained using predictive control.

The advantages of the new stability enhanced backstepping approach are the direct relationship of the controller with the converter dynamic models and the highlight of the variables needed to be measured. Furthermore, the approach uses positive definite Lyapunov functions to guarantee the stability of the system [25–30].

Compared to predictive controllers [31–33] the approach hereafter described requires lower computation power while retaining the response speed of predictive controllers.

The obtained Lyapunov backstepping controllers with stability enhanced are used to control the NPC converter PV voltage, AC currents and the capacitor voltage balance using pulse width modulation with a new dynamic equation of the capacitors incremental unbalance voltage. This paper compares the new stability enhanced backstepping control results with predictive controllers, that optimize the AC currents, capacitor voltage balancing and DC voltage control.

The simulation and experimental results show that the AC currents are almost sinusoidal, the power factor can be made almost unity, and capacitor voltages are balanced. The Lyapunov control method enhances the stability of backstepping controllers for non-linear systems.

The new backstepping control non-linear method has a fast PV voltage control, regarding predictive controllers, allowing the use of this method to quickly adjust the power transfer point of the PV panel to mitigate frequency and voltage variations of the AC microgrid, with reduced computational cost.

This paper presents, in section 2, the multilevel converter model, in the *dq* reference frame, to interface with the PV panel and AC microgrid. New stability enhanced backstepping PWM controllers, to regulate the PV voltage, the AC current, and to balance the capacitor voltages, by adjusting the DC component of the PWM carriers, are then obtained from the converter *dq* model. In section 3, the implementation process of the controlled converter connected to the AC microgrid is described, either at the simulation level in MATLAB / Simulink, or through a low power laboratory prototype. In this section the results are presented, in steady state and transient operation and the performance is evaluated. In the last section, 4, the main conclusions of the paper are presented.

2 AC microgrid model and controllers

Fig. 1 represents the simplified power circuit of the neutral point clamped (NPC) converter, which interfaces the AC microgrid with a PV distributed power source. The voltage U_{pv} is the PV voltage, the current i_{pv} flows from the PV to the microgrid, across the multilevel converter. The AC three-phase currents i_1, i_2, and i_3 flow to the three phases of the AC microgrid, with voltages respectively U_{L1}, U_{L2}, and U_{L3}, using coupling coils, with self-induction coefficient, L, and small internal loss resistor, R. The multilevel converter has two capacitors, C_1 and C_2, with two voltages U_{C1} and U_{C2}, which should be balanced to approximately $U_{pv}/2$. The NPC converter legs can have three states, characterized by the variable γ_k:

$$\gamma_k = \begin{cases} 1 & S_{k1} = 1 \text{ and } S_{k2} = 1 \\ 0 & S_{k1} = 0 \text{ and } S_{k2} = 1 \\ -1 & S_{k1} = 0 \text{ and } S_{k2} = 0 \end{cases} \quad (1)$$

Images are optimised for fast web viewing. Click on the image to view the original version.

Fig. 1

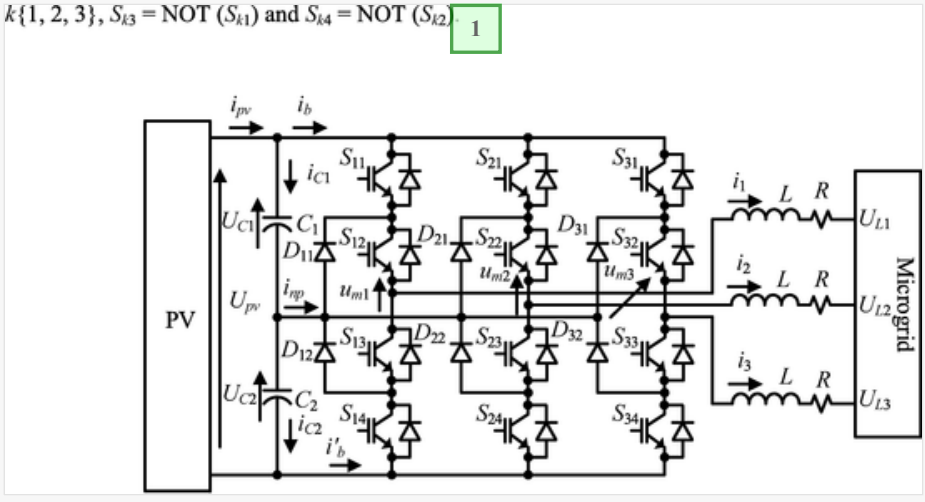

1 Delete the text k{1,2,3}, Sk3 ... {MC COMMENT: Figure correction}

Neutral point clamped converter interfacing PVs to AC microgrid.

with $k, \in\{1, 2, 3\}$, $S_{k3} = \text{NOT}\ (S_{k1})$ and $S_{k4} = \text{NOT}\ (S_{k2})$.

2.1 Neutral point clamped converter model

The AC current equations of the circuit of Fig. 1, in *dq* reference rotating frame, are obtained by applying the Kirchhoff laws, the Clark-Concordia, and Park transforms [34],

$\frac{di_d}{dt} = -\frac{R}{L}i_d + \omega i_q + \frac{\gamma_d}{L}\frac{U_{pv}}{2} - \frac{U_{Ld}}{L}$; (2)

$$\frac{di_q}{dt} = -\omega i_d - \frac{R}{L}i_q + \frac{\gamma_q}{L}\frac{U_{pv}}{2} - \frac{U_{Lq}}{L} \tag{3}$$

The currents i_d and i_q are respectively the averaged values of the direct and the quadrature component the AC converter currents, i_1, i_2, and i_3, in a switching period, ω is the angular frequency of the AC microgrid, γ_d, γ_q, and γ_0 are *dq* transformed switching period averaged values of the semiconductor state variables, γ_1, γ_2, and γ_3, and U_{Ld} and U_{Lq} are the direct and quadrature components of AC voltages of the AC microgrid. It is seen that the dynamics of i_d and i_q although cross-coupled and non-linear can be controlled by γ_d and γ_q, respectively.

The equation describing the dynamic evolution of PV voltage, in *dq* coordinates, is given by:

$$\frac{dU_{pv}}{dt} = -\frac{\gamma_d}{C}i_d - \frac{\gamma_q}{C}i_q + \frac{2}{C}i_{pv} \tag{4}$$

This equation indicates that the variation of the PV voltage depends also on the current i_d and i_q. When the power factor is close to unity the quadrature current i_q is smaller than i_d. In this situation, when the values of the active power, P, are higher than the reactive power values, Q, the current i_d is the dominant term in the control of PV voltage, being i_{pv} considered as a disturbance. In the PV voltage dynamics equation, it was considered that $C_1 = C_2 = C$.

2.2 Design of new stability enhanced backstepping PWM controllers for the PV voltage

Defining the PV voltage error, e_{Upv}, by

$$e_{Upv} = U_{pvRef} - U_{pv} \tag{5}$$

where U_{pvRef} is the PV DC reference voltage. Let V_1 be a Lyapunov function globally positive-definite ($V_1(e_{Upv} \neq 0) > 0$, $V_1(e_{Upv} = 0) = 0$) and radially unbounded ($V_1(|e_{Upv}| \to \infty) \to \infty$ for all e_{Upv}):

$$V_1 = \frac{e_{Upv}^2}{2} \tag{6}$$

For asymptotic stability $\dot{V}_1(e_{Upv} \neq 0) < 0$, therefore it can be written:

$$\frac{dV_1}{dt} = e_{Upv}\frac{de_{Upv}}{dt} = -K_{eUpv}e_{Upv}^2 \tag{7}$$

where K_{eUpv} is a positive definite constant. In the multilevel converter the current i_d is considered the virtual current to control the PV voltage of PV panel. Substituting in (7) the PV voltage error variable, e_{Upv} (5), and the PV voltage dynamics equation, (4), after some manipulation the equation of virtual direct current, i_{dv}, being the reference current to track $i_d = i_{dv}$, is obtained in (8).

$$i_{dv} = \frac{1}{\gamma_{d(t)}} \left(-CK_{eUpv} e_{Upv} - \gamma_q i_q + 2i_{pv} - C \frac{dU_{pvref}}{dt} \right) \quad (8)$$

Where the term γ_d ($\gamma_d \neq 0$) is the control action and will be obtained hereafter, using a new methodology. The i_{pv} current must be measured, the U_{pvref} derivative is usually zero and is multiplied by C, being $C \ll 1$. The gain K_{eUpv} is a positive constant, whose inverse is the time constant of the error decay to zero, as (7) is a first order homogeneous linear differential equation. The product $C\ K_{eUpv}$ should be around 1. The inner current loop (i_{dv} - i_d = 0) reference current i_{dv} is a function of the NPC modulator duty cycle γ_d. To define this duty cycle, an internal feedback loop enforcing $i_d = i_{dv}$ is needed.

To control the current i_d, by the backstepping control method, the current error i_d, e_{id}, is defined by

$$e_{id} = i_{dv} - i_d \quad (9)$$

where i_{dv} is the virtual current obtained in (8). The previous method is recursively applied to the current internal loop. Therefore, a recursively defined positive definite composite Lyapunov function, V_2, adding the squared errors of the U_{pv} voltage and the current i_d, is considered:

$$V_2 = \frac{e_{Upv}^2}{2} + \frac{e_{id}^2}{2} \quad (10)$$

The derivative of V_2 must be negative to ensure stability, being:

$$\frac{dV_2}{dt} = e_{Upv} \frac{de_{Upv}}{dt} + e_{id} \frac{de_{id}}{dt} = -K_{eUpv} e_{Upv}^2 - K_{eid} e_{id}^2 \quad (11)$$

where K_{eUpv} was defined in (7). Replacing in (11) e_{Upv} and e_{id} for (5) and (9), respectively, and using the current dynamic behaviour equation i_d, (2), and the voltage U_{pv}, (4), after considering that there is a tracking error, so that from (9) $i_d = i_{dv} - e_{id}$, and replacing in (11) it is obtained:

$$e_{Upv} \frac{de_{Upv}}{dt} = -K_{eUpv} e_{Upv}^2 - e_{Upv} \frac{\gamma_{d(t)}}{C} e_{id} \quad (12)$$

Using (12) in (11), considering (9) and (2) to simplify $\frac{de_{id}}{dt}$ in (11) it is obtained:

$$\frac{di_{dv(t)}}{dt} + \frac{R}{L} i_d - \omega i_q - \frac{\gamma_{d(t)}}{L} \frac{U_{pv}}{2} + \frac{U_{Ld}}{L} = -K_{eid} e_{id} + \frac{\gamma_{d(t)}}{C} e_{Upv} \quad (13)$$

The $i_{dv(t)}$ current time derivative can be computed as,

$$\frac{di_{dv(t)}}{dt} = -\frac{i_{dv(t)}}{\gamma_{d(t)}} \frac{d\gamma_{d(t)}}{dt} \quad (14)$$

Substituting (14) into (13) the dynamic equation $\frac{d\gamma_{d(t)}}{dt}$ is defined as

$$\frac{d\gamma_{d(t)}}{dt} = \frac{\gamma_{d(t)}}{i_{dv(t)}}\left[K_{eid}e_{id} - \frac{\gamma_{d(t)}}{C}e_{Upv} + \frac{R}{L}i_d - \omega i_q - \frac{\gamma_{d(t)}}{L}\frac{U_{pv}}{2} + \frac{U_{Ld}}{L}\right] \quad (15)$$

the control action $\gamma_{d(t)}$ is obtained by integrating both members of (15) [25]. Assuming the Euler backward finite difference for the $\gamma_{d(t)}$ derivative ($d\gamma_{d(t)}/dt = (\gamma_{d(t+\Delta t)} - \gamma_{d(t)})/\Delta t$) and supposing a discrete control system, with sampling time Δt, that aims to compute γ_d to be applied in the next sampling interval to the PWM generator modulation index, $\gamma_{d(t+\Delta t)}$, it is received:

$$\gamma_{d(t+\Delta t)} = \gamma_{d(t)} + \Delta t\frac{\gamma_{d(t)}}{i_{dv(t)}}\left[K_{eid}e_{id} - \frac{\gamma_{d(t)}}{C}e_{Upv} + \frac{R}{L}i_d - \omega i_q - \frac{\gamma_{d(t)}}{L}\frac{U_{pv}}{2} + \frac{U_{Ld}}{L}\right] \quad (16)$$

Applying the backstepping controller (16) to the NPC converter which is a non-linear system with 27 command combinations defined in (1), the applied command variable $\gamma_{d(t)}$, can be bounded by the limited number of available combinations, therefore not applying $\gamma_{d(t+\Delta t)}$. This limitation on the command variable $\gamma_{d(t)}$ can result in negative values of $\Delta t\frac{\gamma_{d(t)}}{i_{dv(t)}}K_{eid}$, which multiplied by the current i_d error, e_{id}, produces a positive feedback, not observing the Lyapunov stability criteria, the control system becoming unstable.

A new stability enhanced backstepping is here present to overcome the command variable $\gamma_{d(t)}$ limitation. Using the equation in (11) and considering that the control action $\gamma_{d(t+\Delta t)}$, to be applied in the next sampling time ($t + \Delta t$), is related to the control quantity $U_{pv}/2$, always positive, while the voltage error term e_{Upv} computed in the sampling instant t should be evaluated considering the actual value of $\gamma_{d(t)}/C$, it is received:

$$\gamma_{d(t+\Delta t)} = \frac{2}{U_{pv}}\left(L\frac{di_{dv(t)}}{dt} + Ri_d + U_{Ld} - \omega Li_q + LK_{eid}e_{id} - \frac{L}{C}\gamma_{d(t)}e_{Upv}\right) \quad (17)$$

This modification of the original backstepping method approximately introduces some of the integral action present in the exact backstepping method (16), as the next value of the control action $\gamma_{d(t+\Delta t)}$ depends on the actual value of $\gamma_{d(t)}$ times e_{Upv}. Control law (17) also maintains the term $\gamma_{d(t)}/C$ like the exact backstepping method (16) but now with a gain not dependent on the signal of the ratio $\gamma_{d(t)}/i_{dv(t)}$, removing the command variable $\gamma_{d(t)}$ limitations. Using (17) the value of $\gamma_{d(t)}$ to be applied in the next control step, $\gamma_{d(t+\Delta t)}$, depends on its previous value $\gamma_{d(t)}$. Furthermore, the use of the term $di_{dv(t)}/dt$, which can be estimated using the Euler backward finite difference, using the previous values $\gamma_{d(t)}$ and $\gamma_{d(t+\Delta t)}$ is essential to enhance the stability, because the gain $\frac{2}{U_{pv}}LK_{eid}$, that multiply by the i_d current error, e_{id}, is always positive, ensuring the Lyapunov stability. This method reduces the needed processor calculation time comparatively to predictive control. This approach also avoids the division of $\gamma_{d(t)}$ by $i_{dv(t)}$, which could present a negative value, leading to instability.

2.3 Design of PWM backstepping controller for reactive power in AC grid.

To control the i_q quadrature current define the i_q current error, e_{iq}, by

$$e_{iq} = i_{qref} - i_q = -\frac{Q}{U_{Ld}} - i_q \quad (18)$$

where i_{qref} is the reference current depending on the reactive power Q to inject in the AC microgrid. This reference current is zero only if $Q = 0$ (unit power factor). Choosing again a positive definite Lyapunov function, V_3, given by:

$$V_3 = \frac{e_{iq}^2}{2} \tag{19}$$

Writing the time derivative of V_3 and defining the constant K_{eiq} positive the Lyapunov stability criterion is guaranteed.

$$\frac{dV_3}{dt} = e_{iq}\frac{de_{iq}}{dt} = -K_{eiq}e_{iq}^2 \tag{20}$$

Substituting in (20) the current error e_{iq} and using (3), which defines the dynamic behaviour of the current i_q, the reference value for the PWM γ_q index, $\gamma_{q(t+\Delta t)}$, is given in (21),

$$\gamma_{q(t+\Delta t)} = \frac{2L}{U_{pv}}\left(K_{eiq}e_{iq} + \frac{di_{qref}}{dt} + \frac{R}{L}i_q + \omega i_d + \frac{U_{Lq}}{L}\right) \tag{21}$$

2.4 Design of novel backstepping capacitors voltage balancing strategy.

Analysing the circuit of Fig. 1, the dynamic equation of the capacitor's voltage unbalance $e_{UC} = U_{C1} - U_{C2}$ can be written as:

$$\frac{de_{UC}}{dt} = \frac{d\left(U_{C1} - U_{C2}\right)}{dt} = \frac{1}{C}\left(i_b - i_b'\right) = -\frac{1}{C}\left(\gamma_1^2 i_1 + \gamma_2^2 i_2 + \gamma_3^2 i_3\right) \tag{22}$$

Making the variable changes $\gamma_1 \rightarrow \gamma_1 + \Delta_\gamma$, $\gamma_2 \rightarrow \gamma_2 + \Delta_\gamma$, and $\gamma_3 \rightarrow \gamma_3 + \Delta_\gamma$, a novel dynamic equation of the capacitor voltage unbalance (23) of e_{UC} in terms of Δ_γ is obtained:

$$\frac{de_{UC}}{dt} = -\frac{1}{C}\left(\gamma_1 + \Delta_\gamma\right)^2 i_1 - \frac{1}{C}\left(\gamma_2 + \Delta_\gamma\right)^2 i_2 - \frac{1}{C}\left(\gamma_3 + \Delta_\gamma\right)^2 i_3 \tag{23}$$

This variable transformation corresponds to a small DC offset, Δ_γ, in the sinusoidal carriers of the PWM modulator, causing a slight change in the values of semiconductors duty-cycles. The Δ_γ variable introduces a new degree of freedom to dynamic equation of the capacitor voltage to control the balance of these voltages. This transformation of variables also applies to equations (2), (3) and (4), re-written to be represented in the three-phase coordinate system (natural frame of phases 1, 2 and 3). However, the small offset of the carriers Δ_γ multiplied by $i_1 + i_2 + i_3 = 0$, do not change the dynamic equations for the AC currents and PV voltage.

Equation (23) shows that Δ_γ has a negative effect on the capacitor voltage unbalance e_{UC} dynamics, when the AC currents are positive, leading to its convergence to zero. Applying the Clark-Concordia and Park transforms to (23) results, returns the e_{UC} dynamic equation in the *dq* mains frame,

$$\frac{de_{UC}}{dt} = \left(-\frac{2}{C}\gamma_d\Delta_\gamma + \Delta_d\right)i_d + \left(-\frac{2}{C}\gamma_q\Delta_\gamma + \Delta_q\right)i_q \tag{24}$$

In equation (24) the terms that multiply the small offset of the carrier, Δ_γ, are grouped for each current i_d and i_q, that have a gain, $\frac{2}{C}\gamma_d$ and $\frac{2}{C}\gamma_q$. The terms, of currents i_d and i_q, that do not multiply by Δ_γ have been designated components Δ_d and Δ_q, that for control purposes can be considered disturbances, are given by:

$$\Delta_d = \frac{\gamma_d^2 \cos\omega t}{C}\left(\frac{1+\sqrt{12}}{\sqrt{18}}\sin\omega t^2 - \frac{\cos\omega t^2}{\sqrt{6}}\right) + \frac{\gamma_q^2 \cos\omega t}{C}\left(\frac{\sqrt{2}}{6}\cos\omega t^2 - \frac{\sin\omega t^2}{\sqrt{6}}\right) + \frac{\gamma_d\gamma_q \sin\omega t}{C}\left(\frac{4\sqrt{6}+2\sqrt{2}}{6}\cos\omega t^2 - \sqrt{\frac{2}{3}}\sin\omega t^2\right) - \frac{\gamma_d\gamma_0}{C}\frac{2}{\sqrt{3}}; \quad (25)$$

$$\Delta_q = \frac{\gamma_d^2 \sin\omega t}{C}\left(\frac{3}{\sqrt{6}}\cos\omega t^2 - \frac{\sqrt{2}}{6}\sin\omega t^2\right) + \frac{\gamma_q^2 \sin\omega t}{C}\left(\frac{\sin\omega t^2}{\sqrt{6}} - \frac{\sqrt{2}+\sqrt{24}}{6}\cos\omega t^2\right) + \frac{\gamma_d\gamma_q \cos\omega t}{C}\left(\sqrt{\frac{2}{3}}\cos\omega t^2 - \frac{4}{-}\right) \quad (26)$$

From equations (2) and (3), considering steady-state and unit power factor ($i_q = 0$), neglecting the voltage drop across the loss resistance, R, and choosing the dq reference frame so that $U_{Lq} = 0$, the $\frac{2}{C}\gamma_d$, and $\frac{2}{C}\gamma_q$ gains are:

$$\frac{2}{C}\gamma_d = \frac{4U_{Ld}}{CU_{pv}} \quad (27)$$

$$\frac{2}{C}\gamma_q = \frac{4\omega L i_d}{CU_{pv}} \quad (28)$$

Similarly, to the previous cases, a positive definite Lyapunov function V_4 is chosen in (29) and its time derivative is enforced to be negative in (30), being K_{eUC} positive definite.

$$V_4 = \frac{e_{UC}^2}{2} \quad (29)$$

$$\frac{dV_4}{dt} = e_{UC}\frac{de_{UC}}{dt} = -K_{eUC}e_{UC}^2 \quad (30)$$

Replacing in (30) the equation of the dynamic model of the voltage unbalance error of the capacitor voltages (24) gives the control law for the offset of the carriers, $\Delta_{\gamma ref}$:

$$\Delta_{\gamma ref} = \frac{C}{4i_{dc}}\left(K_{eUC}e_{UC} + \Delta_d i_d + \Delta_q i_q\right) \quad (31)$$

2.5 Block diagram of the new stability enhanced backstepping controllers

Fig. 2 shows the block diagram with the PWM new stability enhanced backstepping controllers to connect the PV fed NPC converter to the AC microgrid.

Fig. 2

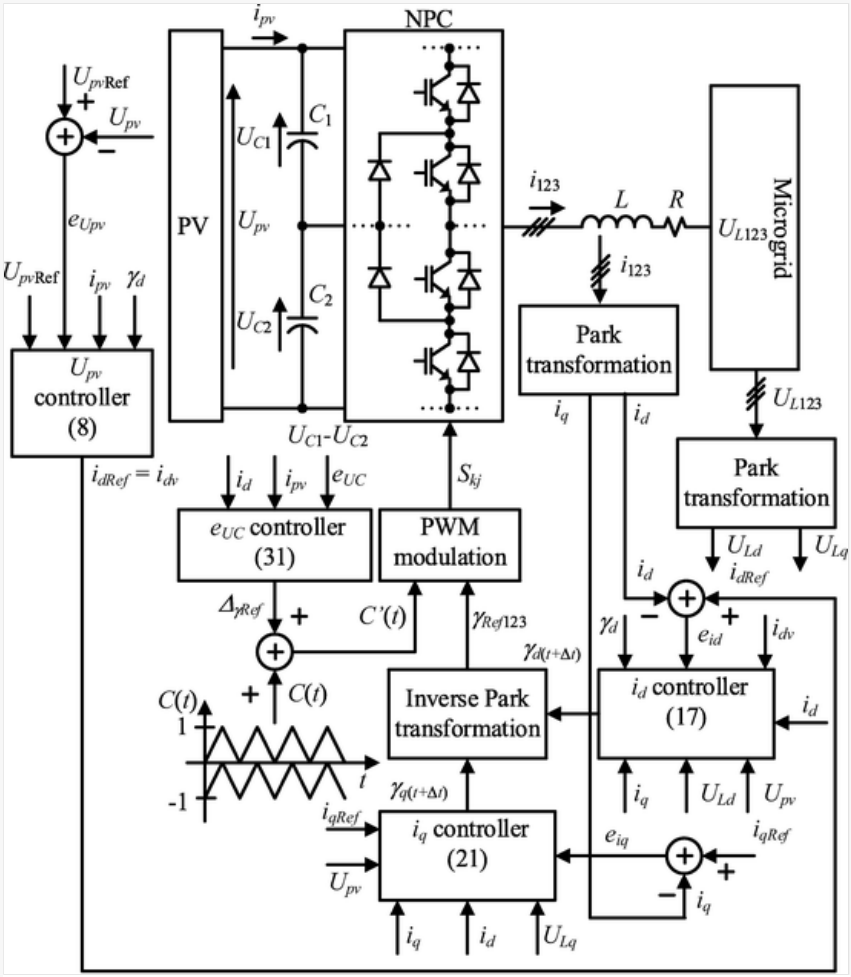

Block diagram of the PV energy conversion new stability enhanced backstepping controller with PWM modulator.

In the block diagram the PV voltage U_{pv} is measured and compared to the reference U_{pvRef}. The application of the new stability enhanced backstepping method to the voltage dynamics equation (4) results in the voltage controller, which calculates the virtual value of the current, i_{dref} in (8), using γ_d and i_{pv}. The AC currents are measured, and the Park transform is applied. These currents in dq, i_d and i_q, are compared with the virtual magnitudes, i_{dv} and $i_{qref} = 0$. The

application of the new stability enhanced backstepping control method results in the control quantities of the converter legs, $\gamma_{d(t+\Delta t)}$ and $\gamma_{q(t+\Delta t)}$, which are then converted to the three-phase coordinate system, γ_1, γ_2, and γ_3. The voltage unbalance of capacitors the control equation (31) is also applied to compute the offset Δ_γ, which is added to the control quantities, γ_1, γ_2, and γ_3, to balance the capacitor voltages.

3 PV fed NPC converter simulation and experimental results

In this section the simulation and experimental results of the PV fed NPC converter interfacing an AC microgrid are presented. The simulations, performed in MATLAB / Simulink, were made based on the microgrid model and the controllers obtained by the new stability enhanced backstepping method. The experimental results were obtained from a laboratory prototype of a PV generator fed multilevel NPC converter connected to an AC low voltage grid (Fig. 1) to experimentally test the performance of the PV fed NPC converter fitted with the obtained backstepping controllers and PWM modulators.

The simulation and experimental results are presented in steady-state and in transient operation. The simulation and experimental results of the new stability enhanced backstepping controllers are compared with predictive controllers. Table 1 lists the parameters and values used in simulation and experimental verification.

Table 1

PV fed NPC converter parameter values.

Parameter	Description	Value
U_{pv}	DC PV voltage	100 V to 140 V
C	Multilevel capacitors	4.4 mF
L	Self-induction coefficient	15.1 mH
R	Loss resistor	0.1 Ω
U_L	AC Line to Line Peak Voltage	60 V
ω	Angular frequency	$2\pi f$
f	AC frequency	50 Hz
K_{eUpv}	PV voltage feedback control gain	127.4
K_{eid}	AC current, direct component, feedback control gain	$30/\Delta t$
K_{eiq}	AC current, quadrature component, feedback control gain	$30/\Delta t$
K_{eUC}	PV voltage capacitor balancing feedback control gain	$2/C$
Δt	Sampling time	28 μs

3.1 PV fed NPC converter steady-state simulation and experimental results

The steady state PV fed NPC converter to AC microgrid simulation of PV voltage are shown in Fig. 3, using a constant PV voltage reference. The results of Fig. 3 (a), with the backstepping controller (16), limiting $\gamma_{d(t)}$ to positive values, show that the PV voltage has a static error 3.0 V, (2.5%), a ripple with approximately 3.1 V RMS and the AC currents show a total harmonic distortion of approximately 13.5% which is not acceptable. The results of Fig. 3(b) with the stability enhanced backstepping controller (17) show that the 3–phase AC currents are balanced and almost sinusoidal, with little total harmonic distortion (THD), 1.7%, and the PV voltage follows the reference with a ripple of approximately 0.1 V RMS and a static error of 0.06 V (0.05 %).

Images are optimised for fast web viewing. Click on the image to view the original version.

Fig. 3

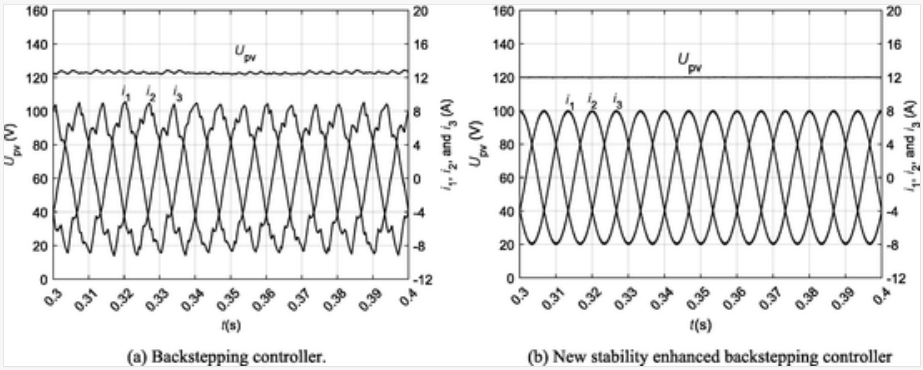

(a) PV voltage, U_{pv}, and AC current, i_1, i_2, and i_3 simulation results in steady state with the backstepping controller (16) and (b) with new stability enhanced backstepping control method (17).

Using (16), results show that the backstepping controller, despite being able to control the PV voltage, albeit with some ripple and static error, presents too much harmonic distortion on the AC currents (Fig. 3 (a)). These results were obtained using a $\gamma_{d(t)}$ positive limiter to guarantee the stability of the system. Increasing the gain K_{eid} improves the results of AC current THD and the PV voltage control. However, this control method cannot be used when the converter is interconnecting hybrid microgrids in which the power transfer direction is bidirectional.

The experimental results of the capacitor voltages and AC current and AC voltage, i_1 and U_{L1}, are shown in Fig. 4. These results show that new stability enhanced backstepping PV voltage controllers, using the novel backstepping control of the capacitors unbalance voltage, with capacitor voltage balance through the offset of the PWM carrier effectively balance the capacitor voltages, Fig. 4 (a). The results obtained are similar to those of the predictive control [17], Fig. 4 (b).

Images are optimised for fast web viewing. Click on the image to view the original version.

Fig. 4

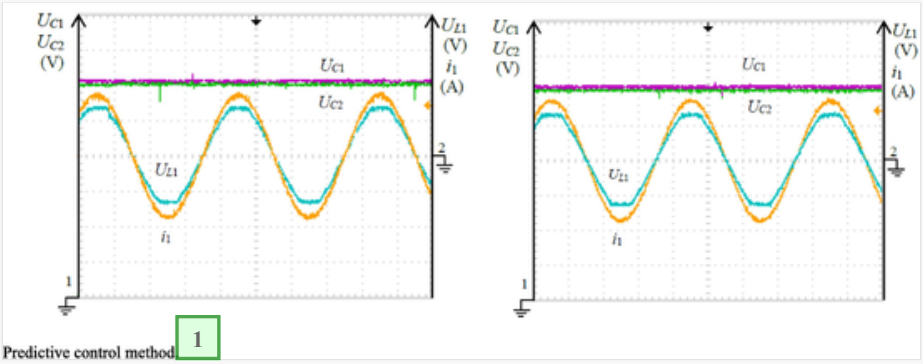

1 Insert: (a) New stability enhanced backstepping PWM control method. (b) Predictive control method. {MC COMMENT: Figure correction}

Experimental results of capacitor voltage, U_{C1} and U_{C2}, AC voltage, U_{L1}, and AC current i_1, in steady state with the new stability enhanced backstepping control method and predictive control method. Vertical: 10 V/div to U_{C1} and U_{C2}, 25 V/div to U_{L1}, and 2.4 A/div to i_1. Horizontal: 5 ms/div.

In steady state, the multilevel converter allowed to connect a PV panel to the microgrid, regulating the PV voltage at an defined point of power transfer. In Fig. 4 the experimental results of the AC current and AC voltage, i_1 and U_{L1}, are

shown, where it can be observed that the power factor is almost unitary.

The steady-state results of the PV fed NPC converter show that the new stability enhanced backstepping control method is able to regulate the PV voltage, the voltage of the capacitors is balanced, the currents are almost sinusoidal, experimental THD is near 1.8%, and the power factor is nearly unitary. Simulation and experimental results are similar.

3.2 PV fed NPC converter results in transient operation

The PV voltage must be regulated to be able to extract maximum power from the PV panel or curtailment of PV might be required to control the power demand of the microgrid. In this subsection, the results of transient the PV fed NPC converter to microgrid operation are shown when there is a PV voltage variation.

Fig. 5 shows the photovoltaic panel power, P_{pv}, as the voltage changes at the terminals of the photovoltaic panel, U_{pv}, having constant solar irradiation. Normally, in electric power networks, a maximum power point transfer algorithm (MPPT) is applied to adjust the U_{pv} voltage value in order to extract the maximum power, point C in Fig. 5. By changing the voltage of the photovoltaic panel, it is possible to curtail the power that is transferred from the photovoltaic panel to an AC microgrid. In Fig. 5 it is observed that the adjustment of the voltage of the photovoltaic panel from 100 V, point A, to 140 V, point B, causes an increase in power transfer of approximately 45%. In a microgrid the adjustment of power transfer of the PV generation provides an additional degree of freedom in the regulation of AC voltage / frequency.

Fig. 5

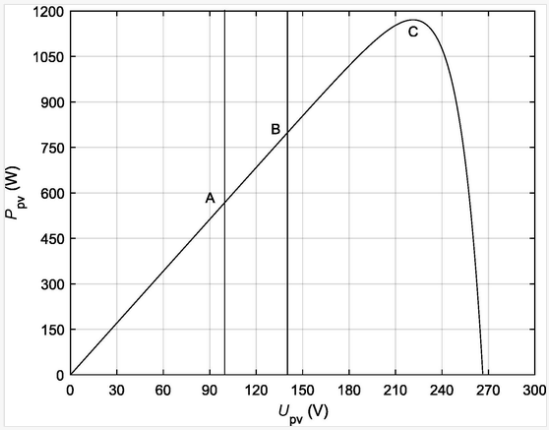

Adjusting the power of the photovoltaic panel, P_{pv}, by changing the panel voltage, U_{pv}, curtailment.

In Fig. 6 the PV voltage experimental results, U_{pv}, are shown when the reference voltage has a linear rising change from 100 V to 140 V. The results in Fig. 6 (a) are obtained using the new stability enhanced backstepping control method and the results in Fig. 6 (b) to the predictive control [17]. The results also show the AC currents during the PV voltage transition.

Fig. 6

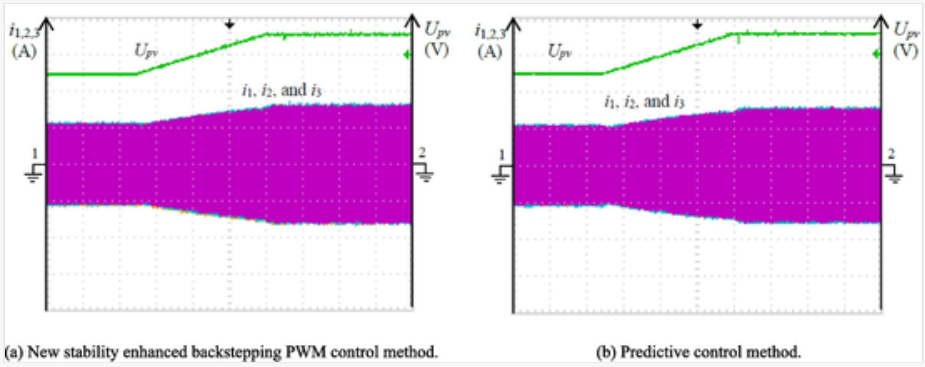

PV voltage and AC currents experimental results in transient mode, when the PV voltage reference change from 100 V to 140 V, with the new stability enhanced backstepping control method and the predictive control. Vertical: 6 A/div and 40 V/div. Horizontal: 0.5 s/div.

These results show that the new stability enhanced backstepping control method controller and the predictive control allowing for the search of the PV panel new operation point to increase the AC power. The new stability enhanced backstepping control method imposes a slew rate of 22.9 V/s on PV voltage while the predictive controller has 24.2 V/s. The power conversion of PV to microgrids, at an intermediate power point, can be used to mitigate AC frequency and voltage disturbances, by positioning the PV voltage using the new stability enhanced backstepping control method, which regulates the power in the microgrid.

In the transient operation the reference PV voltage was changed from 140 V to 100 V and the experimental results are shown in Fig. 7. The results show that the PV voltage transition to the new stability enhanced backstepping PWM control method, Fig. 7 (a), and predictive control method [17], Fig. 7 (b), are similar. The reduction of the PV voltage reference can be used to reduce the AC power, the application of the curtailment effect. This allowing the control of the microgrid AC power and frequency regulation.

Fig. 7

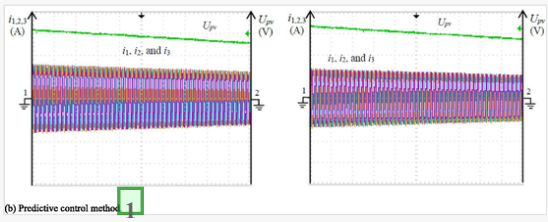

1 Insert: (a) New stability enhanced backstepping PWM control method. (b) Predictive control method. {MC COMMENT: Figure correction}

Experimental results of PV voltage and AC current, i_1, i_2, and i_3, in transient conditions, when the reference is changed from 140 V to 100 V, with the new stability enhanced backstepping control method and the predictive control. Vertical: 6 A/div and 40 V/div. Horizontal: 0.1 s/div.

The NPC converter can be used to connect an AC microgrid to a DC microgrid. In the following experimental results, the new stability enhanced backstepping method regulates the DC microgrid voltage whose DC load is partly supplied by the PV power and the AC microgrid. The NPC converter is transferring power from the AC microgrid to the DC microgrid. The experimental results of Fig. 8 show DC microgrid voltage using the new stability enhanced backstepping control method when variations in DC load power occur. In Fig. 8 (a) the U_{pv} voltage (microgrid DC voltage) and the AC currents, i_1, i_2, and i_3, are shown when the DC load power have a step power increase. At the transition instant (Fig. 8 (a)), the results show that the U_{pv} voltage is almost constant (0.5 % decrease) using the new stability enhanced backstepping. In Fig. 8 (b) the results of DC microgrid voltage and AC currents are shown when the DC load power is decreased. The negative step variation of DC power does not significantly affect the DC microgrid

voltage control (0.5 % increase on DC voltage), of the new stability enhanced backstepping method. These results show that if this converter is connected to a DC microgrid it can regulate the DC microgrid voltage at the connection point when variations in the DC power occur.

Fig. 8

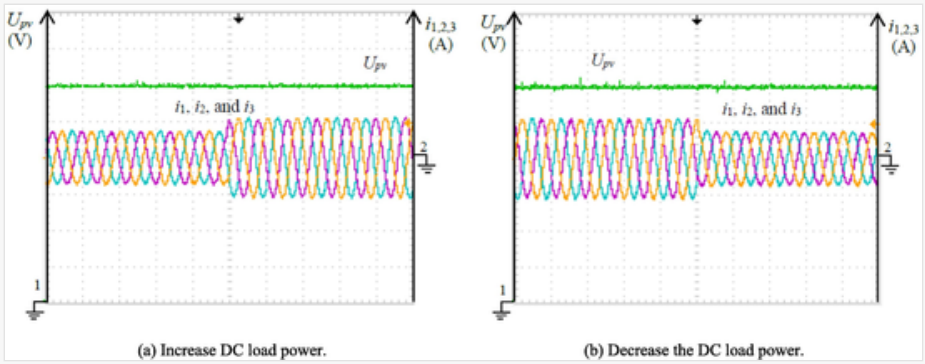

Experimental results of DC microgrid voltage and AC currents, i_1, i_2, and i_3, with the new stability enhanced backstepping method. (a) When increasing the DC load power. (b) When decreasing the DC load power. Vertical: 6 A/div and 20 V/div. Horizontal: 25 ms/div.

In the transient operation, the results do not show visible differences in current control with the new stability enhanced backstepping control method and predictive control method [17], showing that the new stability enhanced backstepping controller have the features of an optimal controller and faster processing time. PV voltage control (or DC microgrid voltage), which gives the reference currents, as is normally done with the control using linear linearized compensators. Simulation and experimental tests were conducted to evaluate the performance of the controllers of capacitor voltages balancing and power factor compensation. The results, in the transient operation, show that the capacitor voltages are balanced, and the power factor is almost unitary. The implementation of the optimal predictive control algorithm in the digital signal processor, dSPACE 1103, requires 678 floating-point operations (flops). For the new stability enhanced backstepping PWM control the number of flops is only 144, a reduction by a factor of near 5 in the computational cost.

4 Conclusions

This paper detailed a new control method for PV fed multilevel neutral point clamped converters, based on a new stability enhanced backstepping method, to be applied in microgrids needing AC currents with low distortion. Multilevel converter dynamics models were presented and used to derive new stability enhanced backstepping controllers. The obtained new stability enhanced controllers contain an implicit integration, being capable of running at frequencies in excess of 35 kHz, due to low computational requirements.

The simulation results in MATLAB / Simulink and experimental results show that the PV voltage of the PV fed NPC converter reference from the MPPT, has similar response in the transient operation (slew rate 5.4% lower), comparatively to an optimal predictive controller, and has little disturbance (0.5 %) when there are sudden variations in the DC load power. The THD of AC currents is very small (1.8%) and the near sinusoidal currents are in phase with the AC voltages, indicating that the converter allows a high-power quality at almost unit power factor if needed. The response of the AC currents, in the transient operation, is much faster than the PV voltage response and the capacitor voltages, whose results show an effective balancing of the capacitor voltages with the new backstepping control of the capacitors unbalance voltage.

The obtained new stability enhanced results also show the power curtailment action as the proposed controller was able to enforce the PV panels operating point to reduce the injected power for AC voltage / frequency regulation with similar results of an optimal predictive controller and with less processing time.

The new stability enhanced backstepping method applied to NPC converter is able to convert power between hybrid microgrids with fast control of DC microgrid voltage, when the DC load have step variations, allowing bidirectional transfer of power between AC and DC microgrids, enhancing the stability of the non-linear NPC converter backstepping method.

Declaration of Competing Interest

The authors declare that they have no known competing financial interests or personal relationships that could have appeared to influence the work reported in this paper.

Acknowledgements

This work was supported in part by national funds through FCT, Fundação para a Ciência e a Tecnologia, under Q5 project UIDB/50021/2020.

Q6 References

The corrections made in this section will be reviewed and approved by a journal production editor. The newly added/removed references and its citations will be reordered and rearranged by the production team.

[1] Guerrero J.M., Chandorkar M., Lee T.-L., Loh P.C. Advanced control architectures for intelligent microgrids—Part I: Decentralized and hierarchical control. IEEE Trans Ind Electron 2012;60(4):1254–1262. doi:10.1109/TIE.2012.2194969.

[2] Hatahet W., Marei M.I., andM. Mokhtar, Adaptive controllers for grid-connected DC microgrids. Int J Electr Power Energy Syst 2021;130:106917. doi:10.1016/j.ijepes.2021.106917.

[3] Yu K., Ai Q., Wang S., Ni J., Lv T. Analysis and optimization of droop controller for microgrid system based on small-signal dynamic model. IEEE Trans Smart Grid 2016;7(2):695–705. doi:10.1109/TSG.2015.2501316.

[4] Liu H., Xie X. Comparative studies on the impedance models of VSC-based renewable generators for SSI stability analysis. IEEE Trans Energy Convers 2019;34(3):1442–1453. doi:10.1109/TEC.2019.2913778.

[5] Armghan H., Yang M., Wang M.Q., Ali N. and Ammar Armghan, “Nonlinear integral backstepping based control of a DC microgrid with renewable generation and energy storage systems”. Int J Electr Power Energy Syst 2020;117:105613. doi:10.1016/j.ijepes.2019.105613.

[6] Silveira J.P.C., Neto P.J.S., Barros T.A.S., Filho E.R. Power management of energy storage system with modified interlinking converters topology in hybrid AC/DC microgrid. Int J Electr Power Energy Syst 2021;130:106880. doi:10.1016/j.ijepes.2021.106880.

[7] Esram T., Chapman P.L. Comparison of photovoltaic array maximum power point tracking techniques. IEEE Trans Energy Convers 2007;22(2):439–449. doi:10.1109/TEC.2006.874230.

[8] Carrasco J.M., Franquelo L.G., Bialasiewicz J.T., Galvan E., Guisado R.C.P., Prats M.A.M., et al. Power-electronic systems for the grid integration of renewable energy sources: A survey. IEEE Trans Ind Electron 2006;53:1002–1016. doi:10.1109/TIE.2006.878356.

[9] Nejabatkhah F., Li Y.W. Overview of power management strategies of hybrid AC/DC microgrid. IEEE Trans Power Electron 2015;30:7072–7089. doi:10.1109/TPEL.2014.2384999.

[10] Salem Q., Xie J. Decentralized power control management with series transformerless H-bridge inverter in low-voltage smart microgrid based P/V droop control. Int J Electr Power Energy Syst 2018;99:500–515. doi:10.1016/j.ijepes.2018.01.047.

[11] Rezaei N., Ahmadi A., Khazali A.H., Guerrero J.M. Energy and frequency hierarchical management system using information gap decision theory for islanded microgrids. IEEE Trans Ind Electron 2018;65:7921–7932. doi:10.1109/TIE.2018.2798616.

[12] Sinha S., Ghosh S., Bajpai P. Power sharing through interlinking converters in adaptive droop controlled multiple microgrid system. Int J Electr Power Energy Syst 2021;128:106649. doi:10.1016/j.ijepes.2020.106649.

[13] Che L., Shahidehpour M., Alabdulwahab A., Turki Y.A. Hierarchical coordination of a community microgrid with AC and DC microgrids. IEEE Trans Smart Grid 2015;6:3042–3051. doi:10.1109/TSG.2015.2398853.

[14] Mortaz E., Valenzuela J. Optimizing the size of a V2G parking deck in a microgrid. Int J Electr Power Energy Syst 2018;97:28–39. doi:10.1016/j.ijepes.2017.10.012.

[15] Hu K.-W., Liaw C.-M. Incorporated operation control of DC microgrid and electric vehicle. IEEE Trans Ind Electron 2016;63:202–215. doi:10.1109/TIE.2015.2480750.

[16] Rodriguez J., Lai J.-S., Peng F.Z. Multilevel inverters: A survey of topologies, controls, and applications. IEEE Trans Ind Electron 2002;49:724–738. doi:10.1109/TIE.2002.801052.

[17] Barros J.D., Silva J.F. Optimal predictive control of three-phase NPC multilevel converter for power quality applications. IEEE Trans Ind Electron 2008;55:3670–3681. doi:10.1109/TIE.2008.928156.

[18] Jayaram N., Agarwal P., Das S. Mathematical model of five-level ac/dc converter in abc reference frame. Int J Electr Power Energy Syst 2014;62:469–475. doi:10.1016/j.ijepes.2014.04.057.

[19] Malakondareddy B., Kumar S.S., Gounden N.A., Anand I. An adaptive PI control scheme to balance the neutral-point voltage in a solar PV fed grid connected neutral point clamped inverter. Int J Electr Power Energy Syst 2019;110:318–331. doi:10.1016/j.ijepes.2019.03.012.

[20] ~~Guilherme Marto Paraíso, Sónia Ferreira Pinto, J F. Silva, "Modelling and nonlinear control of Dual-Active Bridge converters for DC microgrids", IECON 2019-45th Annual Conference of the IEEE Industrial Electronics Society, Volume 1, p 1850-1855, 2019. https://doi.org/10.1109/IECON.2019.8927046.~~Guilherme Marto Paraíso, Sónia Ferreira Pinto, J F. Silva, "Modelling and nonlinear control of Dual-Active Bridge converters for DC microgrids", IECON 2019-45th Annual Conference of the IEEE Industrial Electronics Society, Volume 1, p 1850-1855, 2019. https://doi.org/10.1109/IECON.2019.8927046.

[21] Ezal K., Pan Z., Kokotovic P.V. Locally optimal and robust backstepping design. IEEE Trans Autom Control 2000;45:260–271. doi:10.1109/9.839948.

[22] Dhar S., Dash P.K. A new backstepping finite time sliding mode control of grid connected PV system using multivariable dynamic VSC model. Int J Electr Power Energy Syst 2016;82:314–330. doi:10.1016/j.ijepes.2016.03.034.

[23] Mazenc F., Bliman P.-A. Backstepping design for time-delay nonlinear systems. IEEE Trans Autom Control 2006;51:149–154. doi:10.1109/TAC.2005.861701.

[24]

Davila J. Exact tracking using backstepping control design and high-order sliding modes. IEEE Trans Autom Control 2013;58:2077–2081. doi:10.1109/TAC.2013.2246894.

[25] Martin A.D., Cano J.M., Silva J.F.A., Vázquez J.R. Backstepping control of smart grid-connected distributed photovoltaic power supplies for telecom equipment. IEEE Trans Energy Convers 2015;30:1496–1504. doi:10.1109/TEC.2015.2431613.

[26] Yin X., Zhang W., Jiang Z., Pand L., Lei M. Adaptive backstepping control for maximizing marine current power generation based on uncertainty and disturbance estimation. Int J Electr Power Energy Syst 2020;117:105329. doi:10.1016/j.ijepes.2019.05.066.

[27] Siad S.B., Malkawi A., Damm G., Lopes L., Dol L.G. Nonlinear control of a DC MicroGrid for the integration of distributed generation based on different time scales. Int J Electr Power Energy Syst 2019;111:93–100. doi:10.1016/j.ijepes.2019.03.073.

[28] Chen F., Jiang R., Zhang K., Jiangand B., Tao G. Robust backstepping sliding-mode control and observer-based fault estimation for a quadrotor UAV. IEEE Trans Ind Electron 2016;63:5044–5056. doi:10.1109/TIE.2016.2552151.

[29] de Oliveira G.C., Damm G., Monaro R.M., Lourenço L.F.N., Carrizosa M.J., Lamnabhi-Lagarrigue F. Nonlinear control for modular multilevel converters with enhanced stability region and arbitrary closed loop dynamics. Int J Electr Power Energy Syst 2021;126:106590. doi:10.1016/j.ijepes.2020.106590.

[30] Linares-Flores J., García-Rodríguez C., Sira-Ramírez H., Ramírez-Cárdenas O.D. Robust backstepping tracking controller for low-speed PMSM positioning system: Design, analysis, and implementation. IEEE Trans Ind Inf 2015;11:1130–1141. doi:10.1109/TII.2015.2471814.

[31] Ni F., Zheng Z., Xie Q., Xiao X., Zong Y., Huang C. Enhancing resilience of DC microgrids with model predictive control based hybrid energy storage system. Int J Electr Power Energy Syst 2021;128:106738. doi:10.1016/j.ijepes.2020.106738.

[32] Barros J.D., Silva J.F.A., Jesus É.G.A. Fast-predictive optimal control of NPC multilevel converters. IEEE Trans Ind Electron 2013;60:619–627. doi:10.1109/TIE.2012.2206352.

[33] Calle-Prado A., Alepuz S., Bordonau J., Cortes P., Rodriguez J. Predictive control of a back-to-back NPC converter-based wind power system. IEEE Trans Ind Electron 2016;63(7):4615–4627. doi:10.1109/TIE.2016.2529564.

[34] Pires V.F., Fialho J., Silva J.F. HVDC transmission system using multilevel power converters based on dual three-phase two-level inverters. Int J Electr Power Energy Syst 2015;65:191–200. doi:10.1016/j.ijepes.2014.10.002.

Highlights

- A new backstepping controllers with enhanced stability to deliver energy from ~~photovoltaic (~~PV~~)~~ panels into AC microgrids is proposed.

- The PV power curtailment to the AC microgrid provides an ~~additional~~ extra degree of freedom in the regulation of AC voltage / frequency.
- Novel ~~dynamic~~ equation of the capacitors incremental unbalance voltage for ~~neutral point clamped (~~NPC~~)~~ converters is used to design backstepping ~~pulse width modulation (PWM)~~ controller.
- The ~~PWM stability enhanced~~ backstepping control reduces the computational cost comparatively predictive controllers with similar power quality.

Queries and Answers

Q1

Query: Please review the **given names and surnames** to make sure that we have identified them correctly and that they are presented in the desired order. Carefully verify the spelling of all authors' names as well. If changes are needed, please provide the edits in the author section. /

Answer: Reviewed

Q2

Query: Your article is being processed as a regular item to be included in a regular issue. Please confirm if this is correct or if your article should be published in a special issue using the responses below. /

Answer: Yes

Q3

Query: Highlights are 3–5 bullet points, no more than 125 characters per bullet point. Please provide it in correct format. For more information, see www.elsevier.com/highlights. /

Answer: A new backstepping controllers with enhanced stability to deliver energy from PV panels into AC microgrids is proposed.
The PV power curtailment to the AC microgrid provides an extra degree of freedom in the regulation of AC voltage / frequency.
Novel equation of the capacitors incremental unbalance voltage for NPC converters is used to design backstepping controller.
The backstepping control reduces the computational cost comparatively predictive controllers with similar power quality.

Q4

Query: As per the journal style, maximum of 6 keyword(s) is/are only allowed. Kindly check which 6 keyword(s) has/have to be retained. /

Answer: Energy conversion; PV; Microgrids; Stability enhanced backstepping controller; NPC; Pulse width modulation.

Q5

Query: Correctly acknowledging the primary **funders and grant IDs** of your research is important to ensure compliance with funder policies. Please make sure that funders are mentioned accordingly. Fundação para a Ciência e a Tecnologia, Portugal? /

Answer: Reviewed

Q6

Query: Please note that we matched the supplied reference content against the Crossref.org database and provided required missing information in the output. Kindly check the output of all the references. /

Answer: [20] Guilherme Marto Paraíso, Sónia Ferreira Pinto, J F. Silva, “Modelling and nonlinear control of Dual-Active Bridge converters for DC microgrids”, IECON 2019-45th Annual Conference of the IEEE Industrial Electronics Society, Volume 1, p 1850-1855, 2019. https://doi.org/10.1109/IECON.2019.8927046.